Cancer Imaging (2013) **13(4),** 645–657
DOI: 10.1102/1470-7330.2013.0057

REVIEW

Yttrium-90 radioembolization of liver tumors: what do the images tell us?

Pavel Singh, Gopinathan Anil

Department of Diagnostic Imaging, National University Hospital and Yong Loo Lin School of Medicine, National University of Singapore, Singapore

Corresponding address: Gopinathan Anil, Department of Diagnostic Imaging, National University Hospital, 5 Lower Kent Ridge Road, Singapore 119288.
Email: ivyanil10@gmail.com

Date accepted for publication 12 December 2013

Abstract

Transarterial radioembolization (TARE) with yttrium 90 microspheres is an increasingly popular therapy for both primary and secondary liver malignancies. TARE entails delivery of β-particle brachytherapy and embolization of the tumor vasculature. The consequent biological sequelae are distinct from those of other transarterial therapies for liver tumors, as reflected in the often baffling post-treatment imaging features. As the clinical use of TARE is increasing, more diverse post-treatment radiological findings are encountered with variable overlap among treatment response, residual disease, reactionary changes and complications. Thus, post-TARE image interpretation is challenging. This review provides a comprehensive description of the different findings seen in post-treatment scans, with the aim of facilitating appropriate radiological interpretation of post-TARE pathologic changes, notwithstanding their existing limitations.

Keywords: *Hepatic tumors; multimodality imaging; yttrium 90 radioembolization.*

Introduction

In patients with primary or metastatic liver malignancy, in the absence of disseminated disease, maximum survival benefit can be achieved through surgical resection, with or without adjuvant chemotherapy. However, most hepatic malignancies are inoperable at presentation as well as at recurrence. For such patients, locoregional treatments (LRT) offer a reasonable therapeutic option before palliative chemotherapy or best supportive care. Among the LRTs, transarterial therapies are especially useful in treating patients with multifocal and extensive disease that is restricted to the liver. These transarterial therapies exploit the dual blood supply of the liver[1]. Hepatocellular carcinomas (HCC) receive most of their blood supply from hepatic arteries unlike the normal liver, which depends on the portal vein for more than 75% of it perfusional requirements. Even hepatic metastases >3 mm derive 80–100% of their blood supply from the hepatic arterial rather than the portal venous circulation[2]. Moreover, the density of arterial vessels around a metastatic lesion is estimated to be 3 times more than in normal liver tissue[3]. For these reasons, if radioactive microspheres are released into the hepatic artery, the bulk of the dose preferentially reaches the tumor as opposed to the normal liver. Microspheres that are 20–40 μm in size are optimal for this purpose because they are small enough to reach the arteriolar network in and around the tumor but too large to freely cross over through the capillary network (usually 8–10 μm in size) into the venular side[3].

The high radiosensitivity of normal hepatocytes renders the liver unsuitable for external radiotherapy. The dose required to destroy solid tumors, estimated at 70 Gy, is far greater than the hepatic tolerance dose of 35 Gy, when delivered to the whole liver in fractions of 1.8 Gy/day[4]. However, the technique of selective internal radiotherapy (SIRT) permits delivery of tumoricidal doses of radiation to the hepatic tumors without causing significant damage to normal parenchyma. SIRT involves transarterial radio-embolization (TARE) with a high-energy radiation source bound to an appropriate embolization particle. In the last decade, TARE with yttrium 90 (^{90}Y) microspheres has become popular in the treatment of

This paper is available online at http://www.cancerimaging.org. In the event of a change in the URL address, please use the DOI provided to locate the paper.

1470-7330/13/000001 + 13

both primary and secondary liver tumors. ^{90}Y is a pure β emitter with a short half-life of 64 h, high average energy (0.936 MeV) and limited tissue penetration (mean 2.5 mm, max 11 mm), making it an ideal transarterial liver-directed agent. Once lodged in the arterioles, ^{90}Y particles are capable of delivering an intense local radiotherapeutic effect (from 50 to >1000 Gy) to the target areas[5]. The embolic effect of tumor devascularization by the carrier microspheres is variable; it depends on the type of microsphere (glass or resin) used, the nature of the tumor being treated and the background status of the liver. Several cohort studies have reported an impressive response to treatment and survival benefit from TARE with ^{90}Y microspheres in both primary and metastatic hepatic neoplasms[6–9]. TARE also has the potential to be used synergistically to facilitate curative surgery[6].

The clinical outcome of a technically successful TARE should be ascertained before making further therapeutic decisions. Histopathologic examination and measuring survival advantage are the best ways to confirm the clinical success of a tumoricidal treatment, but they are not feasible options for guiding short- to intermediate-term clinical decision making. In practice, these decisions are largely guided by the radiological response to treatment. With the combined effects of radiation and embolization, the post-therapy imaging findings can be different and more variable than those seen with other transarterial therapies. Hence, a complete understanding of the possible post-treatment changes is essential for a meaningful radiologic follow-up of patients who have undergone TARE. This review provides a comprehensive description of the different findings seen in post-treatment scans, with that aim of facilitating appropriate radiologic interpretation of post-TARE pathologic changes, not withstanding their existing limitations.

Assessment of tumor response

In cancer therapy, the primary tool of response assessment is survival; nonetheless, tumor response is a pivotal surrogate marker for treatment efficacy. The traditional World Health Organization (WHO) and Response Evaluation Criteria in Solid Tumors (RECIST) criteria for measuring reduction in tumor size were designed for assessing cytotoxic agents and hence they are not entirely appropriate for assessing LRTs such as TARE[10,11]. For LRTs, apart from standard size criteria, response can also be evaluated using other aspects such as tumor necrosis, reduction in tumor vascularity, reduced metabolic activity on fluorodeoxyglucose (FDG)-positron emission tomography (PET) and changes seen on functional magnetic resonance imaging (MRI)[12,13]. The WHO and RECIST criteria do not take into account antitumor activity other than tumor shrinkage; hence, they tend to underestimate the response to LRTs. In comparison, the European Association for the Study of the Liver (EASL) criteria that were originally described for HCC provide a better reflection of post-treatment residual viable tumor[14]. It recommends estimation of viable tumor area based on contrast-enhanced radiologic imaging. In a study involving 42 patients with HCC treated with ^{90}Y microspheres, objective response (OR) was seen in 23% of patients when assessed with RECIST criteria and in 59% with EASL criteria[15]. Another study evaluating hepatic metastasis from colorectal cancer, also found that a combination of size and necrosis criteria may be more accurate than size criteria alone in the assessment of objective response to TARE[16]. In a similar study of 30 patients with HCC and hepatic metastasis who underwent TARE, the OR rate was 24%, 31%, and 72% with WHO, RECIST, and EASL criteria, respectively[17]. The concept of viable tumor introduced by EASL was subsequently endorsed by the American Association for the Study of Liver Disease (AASLD). In 2008, the AASLD-Journal of the National Cancer Institute guidelines formally introduced the concept of viable tumor and tumor necrosis in response assessment using the RECIST criteria; this amended version is referred to as the modified RECIST (mRECIST) criteria[18].

Post-TARE imaging generally begins with contrast-enhanced computed tomography (CT), MRI, and/or PET/CT. This should preferably match the pre-treatment imaging in modality and technique. The initial post-treatment imaging is usually at 1 month after treatment, and is followed by serial examinations every 3 months[19]. Although response to treatment evolves gradually, early imaging is important to identify the non-responders who tend to have poor survival. This is especially relevant when the procedure is being done in a staged manner.

Tumor response

Change in tumor size and necrosis

Traditionally, response to treatment is assessed as a decrease in the size of the tumor[10,11]. However, after TARE, the tumor may shrink, remain the same, or even increase in size (Figs. 1–3). Treatment-related necrosis, edema, and hemorrhage may cause an initial increase in the size of a tumor that is otherwise responding to therapy[20]. Such an increase in size of the target lesion with no enhancement is usually seen at a mean interval of 29–31 days after TARE[15,21]. This finding may persist for several months. The presence and extent of tumor necrosis should be taken into consideration for accurate measurement of residual tumor. Post-radioembolization coagulative necrosis is seen as a non-enhancing area on a CT scan with less than 10 HU change in attenuation after contrast administration[15,16]. It is not unusual to find well-defined small necrotic areas on post-treatment imaging with no corresponding lesion on the pre-treatment scan. This represents necrosis of the small volume tumors that were not detectable on pre-treatment imaging. In responding tumors, the median time to response is

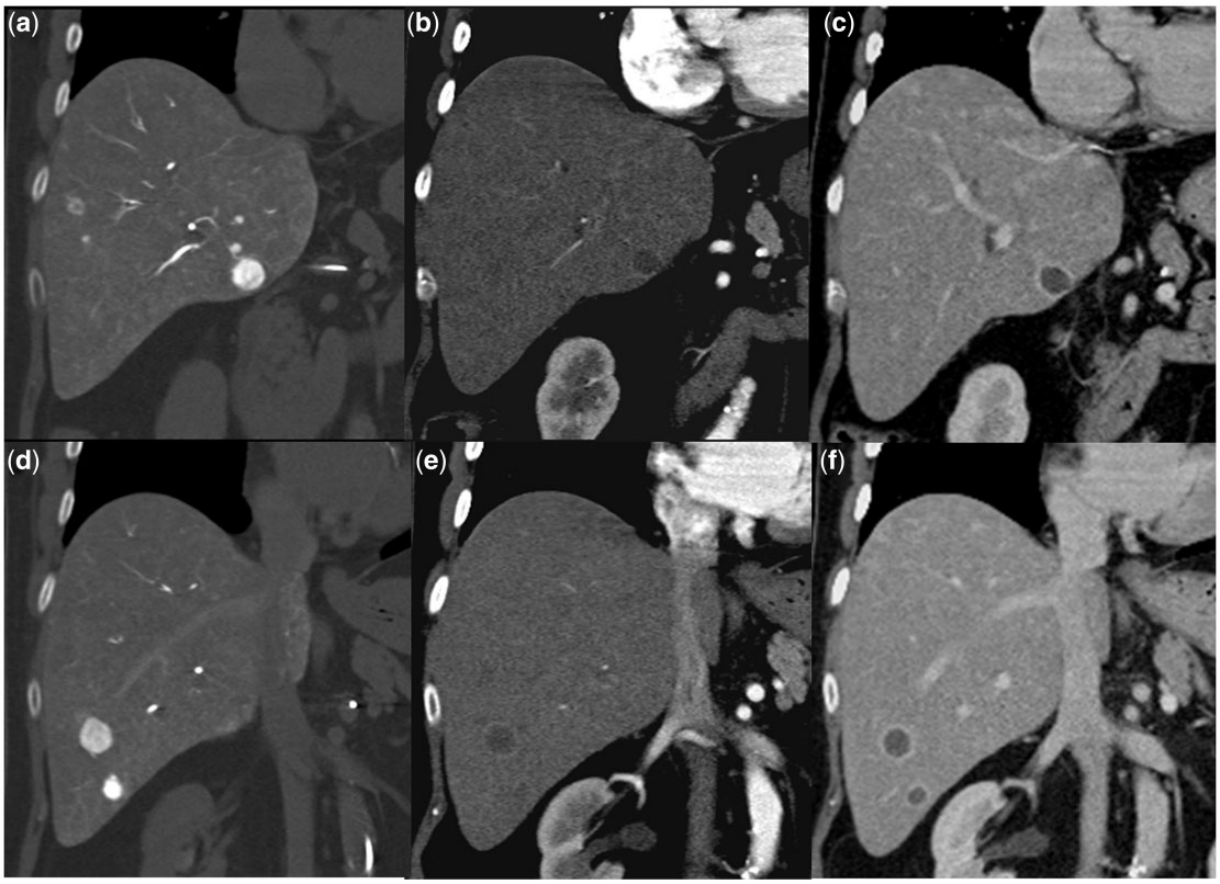

Figure 1 **Pre-treatment arterial phase CT scan (1a and 1b) shows multiple hypervascular hepatomas. Two months after TARE, the follow-up scan in the arterial phase (1c and 1d) and venous phase (1e and 1f) shows stable size of the tumors, but they are completely necrotic with reactionary rim enhancement.**

118–120 days when assessed using size as the only criteria, 29–30 days by necrosis as the only criteria and 31–34 days using combined (size and necrosis) criteria[15,16]. In practice, rather than complete necrosis of all the treated tumors, patchy necrosis with variable residual enhancing areas in many of them is the more frequently encountered picture. Such changes are often seen between 7 and 30 days and may persist for many months. When seen in the early follow-up scans, this appearance does not have a predictive value. However, if it persists after 90 days, especially with arterial phase enhancement, it most likely represents residual disease[21]. An eccentric enhancing nodule in a treated lesion is more likely to represent residual disease. When Keppke et al.[15] found such nodules with a mean thickness of 17 mm, at a mean interval of 55 days after treatment, more than 70% of them resulted in progressive disease, a few remained stable and a small minority resolved without further treatment.

Reduction in tumor vascularity

In patients responding to TARE, there will be reduction/elimination of tumor vascularity. This is a well-accepted clinical end point in the assessment of response to transcatheter arterial chemoembolization (TACE) and is also applicable in patients who have received ^{90}Y therapy. Loss of vascularity may or may not be accompanied by non-enhancing hypodensity on CT scan (usually interpreted as necrosis as shown in Figs. 1–3). It may manifest as complete disappearance of a tumor with no residual stigmata, especially in small lesions. For hypervascular tumors, resolution of the hypervascularity with the tumor-bearing areas showing enhancement and morphology similar to background hepatic parenchyma should be considered a favorable response[21] (Fig. 4).

Metabolic activity on FDG-PET

Liver metastases are generally FDG avid and hence PET/CT with FDG has been found to be equal or superior to both CT and MRI for detecting them[22]. After LRT, PET/CT has been found to be valuable for differentiating residual metastasis from benign post-therapy findings[23]. Reduction in FDG uptake after ^{90}Y microsphere therapy is well described in the literature[16,20,24] (Fig. 5). As PET/CT is a cost and resource intensive imaging modality, its routine use in post-TARE follow-up is not

Figure 2 **Pre-treatment arterial phase CT scan (2a and 2b) shows an enhancing mass in the right lobe of the liver. The follow-up scan performed 4 weeks after TARE (2c and 2d) demonstrates an increase in tumor size but more than more than 80% of its volume is necrotic with the only viable tumor seen as a nodular enhancing area along its inferomedial margin. Despite of the increase in tumor size, this qualifies as a favorable response to treatment.**

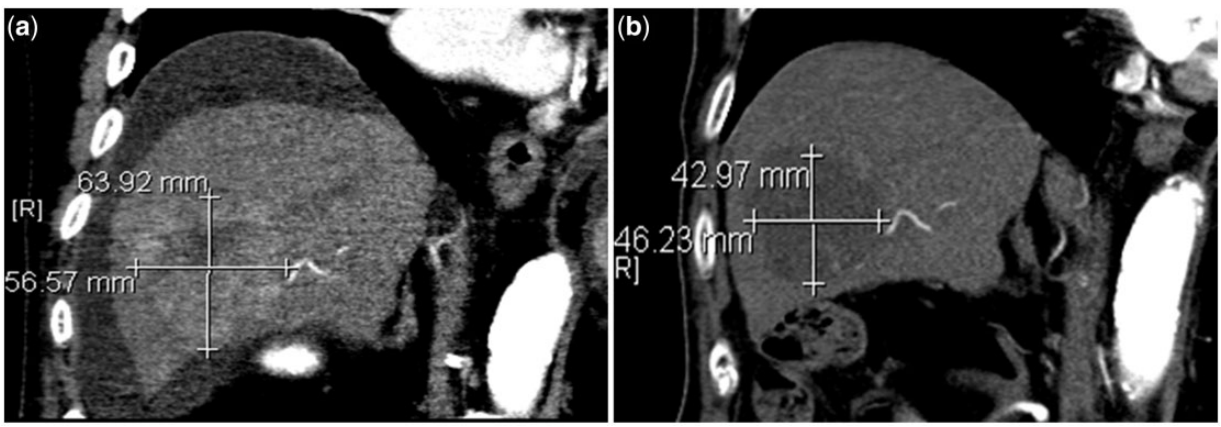

Figure 3 **The pre-TARE (3a) and post-TARE (3b) arterial phase CT scans show complete necrosis of a hypervascular hepatoma with modest decrease in tumor size, consistent with complete response.**

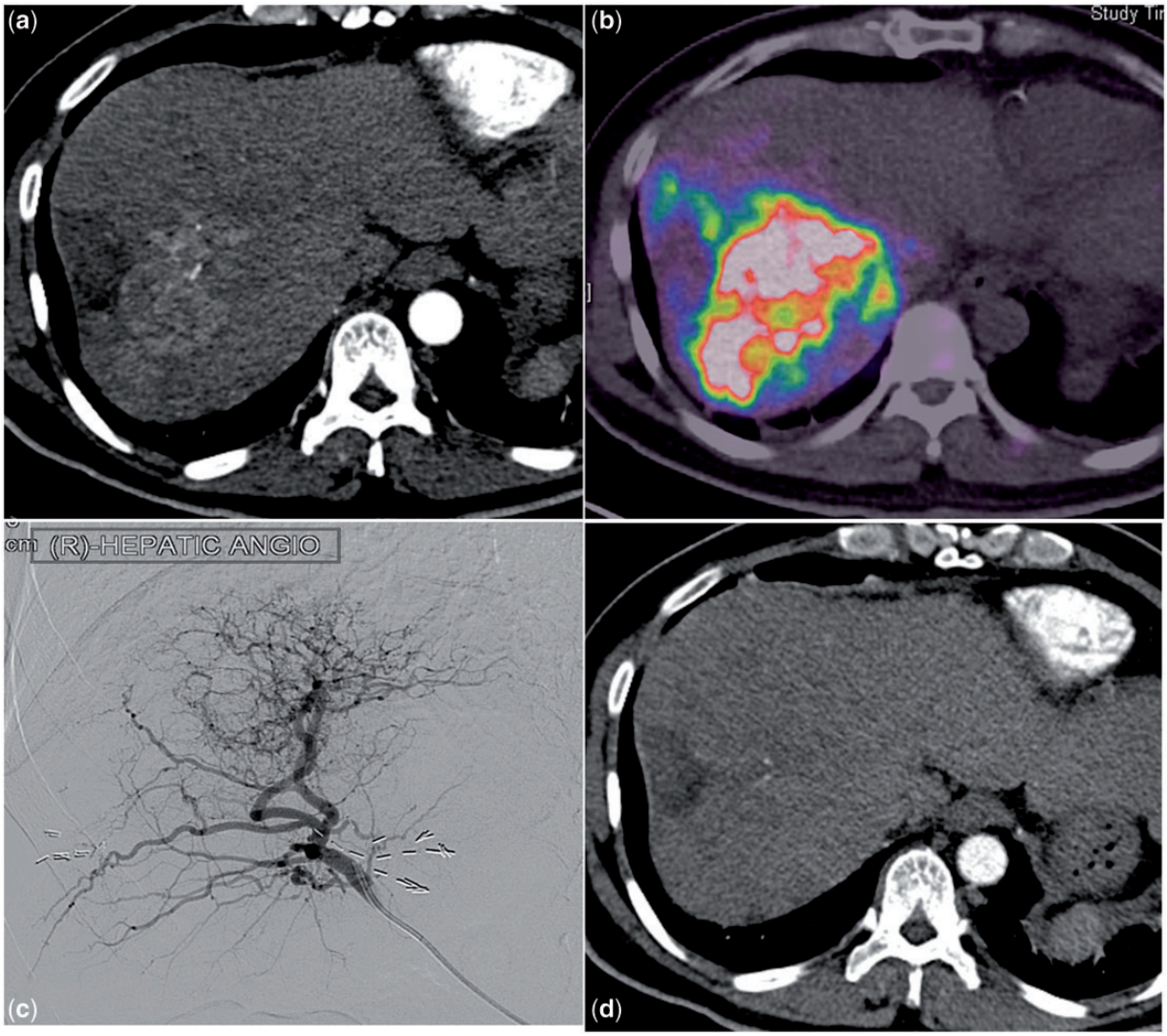

Figure 4 **Local recurrence of a previously resected, poorly differentiated hepatoma is seen as an ill-defined infiltrative enhancing mass in segment 7 and 8 of the liver, on arterial phase CT (4a). The tumor is FDG avid on PET/CT (4b) and markedly hypervascular with multiple, tortuous feeding arteries on angiography (4c). The CT scan done 2 months after TARE (4d) shows complete response with no discrete area of necrosis or any other stigmata of the tumor.**

prevalent. In our practice, PET/CT is reserved as a troubleshooter in differentiating viable neoplastic tissue from edema, hemorrhage or fibrosis after treatment of hepatic metastases. In patients with hypovascular liver metastases, Miller et al.[16] found that PET could detect post-^{90}Y response earlier than the CT and MRI (Fig. 5). However, this role cannot be extrapolated to assessment of patients who have received TARE for HCC. Compared with contrast-enhanced CT, the sensitivity of FDG-PET in the diagnosis of primary HCC is poor (55% vs 90%)[25]; this observation can be explained by the poor FDG avidity of well-differentiated HCC with only poorly differentiated hepatomas accumulating FDG. Dual tracer PET/CT using both FDG and [^{11}C]acetate (the latter accumulates in low-grade HCC) may potentially be useful for detecting post-TARE residual HCC; however, this role has not yet been established.

Diffusion-weighted MR imaging

Anatomic assessment of tumor size may be limited by the inability to differentiate transient increase in tumor size due to post-treatment edema from progressive disease[26]. Similarly, post-TARE enhancement of a tumor can represent viable tumor or post-treatment granulation tissue[27]. Hypovascular tumors are especially difficult to assess for response because CT and MRI rely heavily on post-contrast enhancement to identify residual tumor. In such circumstances, the functional MRI technique of diffusion-weighted imaging (DWI) may be useful (Fig. 6). DWI detects alterations in the motion of water molecules resulting from compromised cell membrane integrity or edema. The diffusion of water molecules is quantified by measuring apparent diffusion coefficient (ADC) values. The high cellular density of tumors leads to restricted

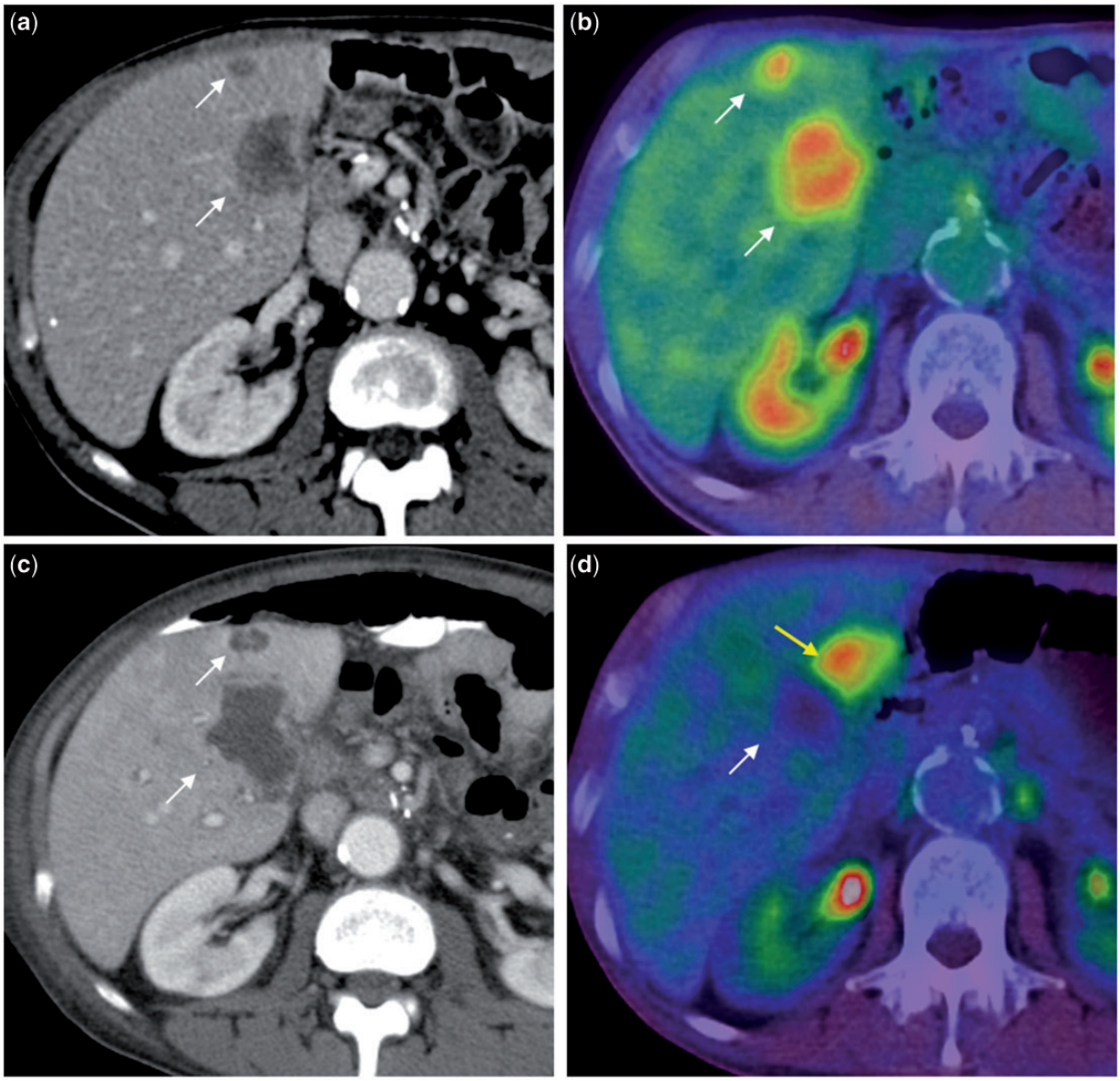

Figure 5 **Contrast-enhanced CT scan (5a) shows two hypodense metastases (white arrows) that are FDG avid on PET/CT (5b). In the follow-up CT scan done 2 months after TARE (5c), they are larger in size with reactive rim enhancement and no internal enhancement. This was interpreted as complete necrosis of these metastases and confirmed with a concomitantly performed PET/CT scan (5d) that shows no FDG uptake in the treated lesion (white arrow); however, a new hypermetabolic focus (yellow arrow) is noted adjacent to the treated lesion that is not visible on the contrast-enhanced CT scan (5c). This illustrates the superiority of functional over morphological imaging in the evaluation of hepatic metastases after radioembolization.**

diffusion of water molecules and hence lower ADC values. After treatment, there is breakdown of cell membranes, which leads to increased ADC values. DWI may assist in early determination of the success or failure of ^{90}Y therapy. In patients who had received radioembolization for HCC, Rhee et al.[28] found that tumor response assessed with DWI at 1 month preceded anatomic size changes at 3 months. By evaluating ADC values, diffusion-weighted MRI has been able to detect tumor response accurately within 42 days of TARE[29].

Benign post-treatment findings

Peritumoral edema

Peritumoral edema is a known radiologic finding after TARE with ^{90}Y microspheres. No definitive pathologic basis has been identified; presumably these changes are secondary to the intense surrounding inflammatory reaction caused by the radiation therapy[30]. As discussed earlier, the apparent increase in tumor size due to

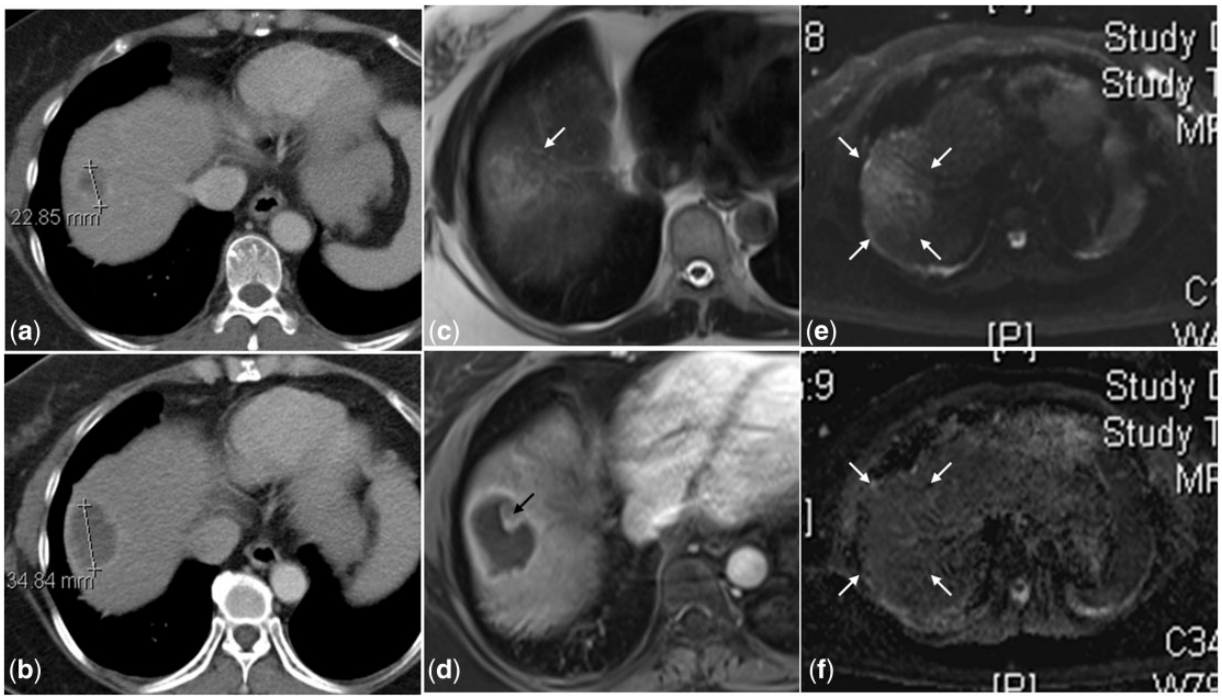

Figure 6 **A hypodense metastatic lesion is seen at the dome of the right lobe in the pre-treatment CT scan (6a) that is larger in size and continues to be hypodense at 1 month after TARE (6b). Due to the inherent hypovascularity of the tumor, it is difficult to ascertain if this represents tumor progression or necrosis. On MRI, the lesion is heterogeneous and hyperintense on the T2-weighted image (6c) with only rim enhancement on the post-gadolinium T1-weighted image (6d) suggestive of internal necrosis. The superior soft tissue resolution of MRI also depicts an eccentric solid nodule (black arrow in 6d) along the margin of this necrotic lesion that is not visible on the CT scan (6b). This indeterminate nodule shows no diffusion restriction on the diffused-weighted (6e) and ADC (6f) images, confirming the absence of any residual disease.**

peritumoral edema may need correlation with functional or metabolic imaging to distinguish it from disease progression[30,31] (Figs. 5 and 6). With diffusion-weighted MRI, post-TARE inflammatory changes can be differentiated from viable tumor, because the former allows free movement of water molecules. Peritumoral edema is transient but can persist for 3–6 months after therapy[31].

Rim enhancement

A thin rim (less than 5 mm in thickness) of enhancement around a treated lesion is a common finding after ^{90}Y therapy[15] (Figs. 1 and 6). Smooth and uniform rim enhancement usually represents granulation tissue around the tumor undergoing radiation necrosis. Keppke et al.[15] found such enhancement in one-third of patients who underwent ^{90}Y therapy; 80% of them responded to treatment and 13% had stable disease. The mean time for appearance and resolution of such rim enhancement was 52 and 131 days, respectively. Kulik et al.[32] observed a high correlation between the radiologic finding of peripheral ring enhancement and complete pathologic necrosis of the tumor in the explant specimens from 20 patients who were either bridged or downstaged to resection or transplantation with TARE.

Ill-defined geographic areas of hypoattenuation

In the portovenous phase of the CT scan, around 40% of patient who have had ^{90}Y therapy may show ill-defined, geographic, hypoattenuating areas in a previously normal liver parenchyma (Fig. 7). These areas generally correspond to the vascular territory of a treated segment or lobe. They are often periportal and perilesional in distribution. There is no mass effect and blood vessels can be seen traversing these hypodense areas. This radiologic finding has no known clinical significance and no loss of hepatic function is attributable to it. Miller et al.[16] found such changes between 22 and 132 days after treatment (mean, 60 days), and all of them showed varying degrees of resolution between 36 and 158 days (mean, 81 days); in 37% of the patients these changes resolved completely. This benign finding can mimic progressive infiltrative tumor and its presence in the background makes assessment of tumor response more challenging.

The exact pathogenesis of the above finding is unknown. Studies on canine models have shown edema, congestion, and microinfarction in liver parenchyma after intra-arterial radiotherapy[33]. The same

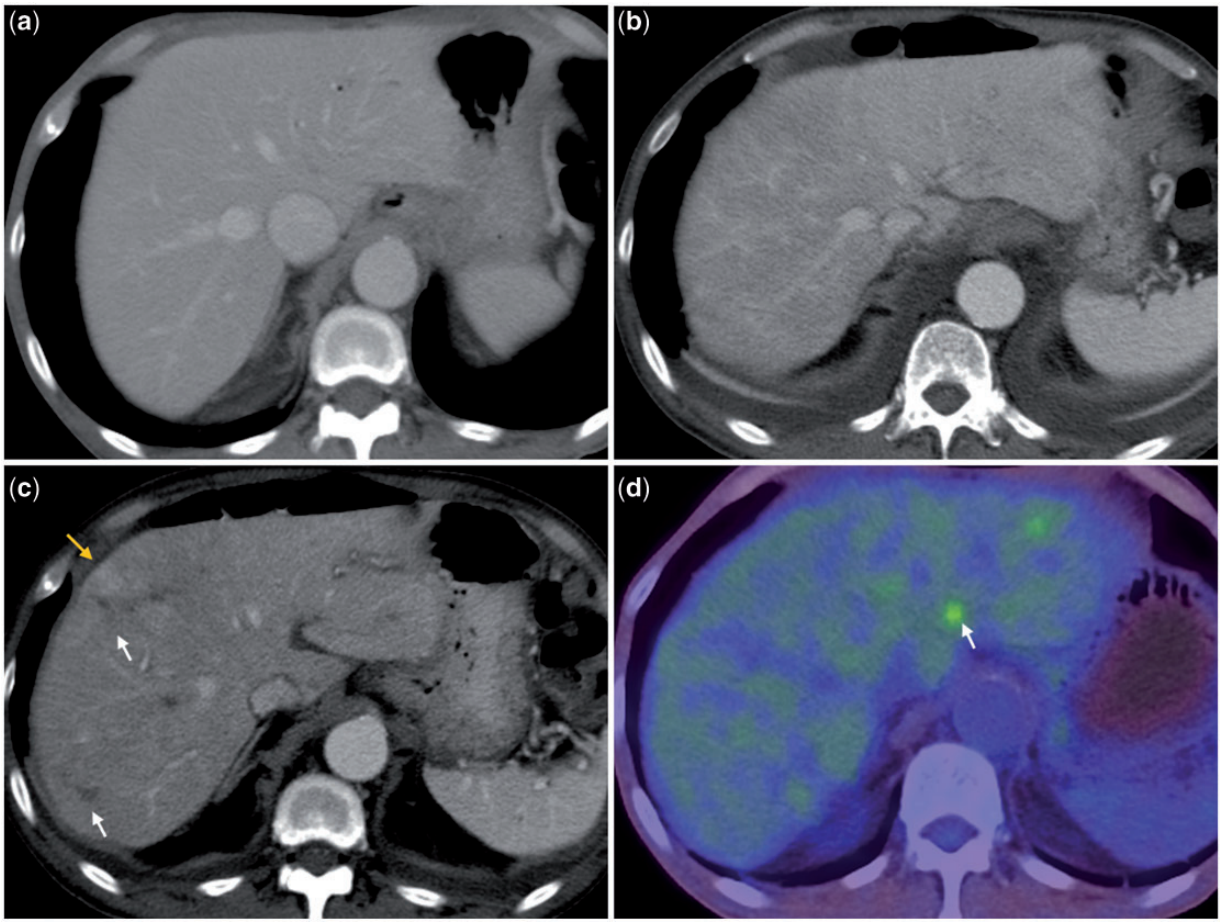

Figure 7 **Pre-treatment portovenous phase CT scan (7a) shows homogenous attenuation of the hepatic parenchyma. One month after unilobar radioembolization (for hepatic metastases from pancreatic carcinoma) to the right lobe, in the portovenous phase CT images (7b and 7c), the right lobe is heterogeneously hypodense whereas the naive left lobe continues to have a homogeneous attenuation. Ill-defined hypodense (white arrow in 7c) and hyperdense (yellow arrow in Fig. 7c; this is probably an island of normal liver) areas with no mass effect are seen in the treated lobe. These post-TARE changes can be confused with diffuse infiltrative disease. A PET/CT scan done 1 month later (7d) confirms the benign nature of these changes. Note the hypermetabolic focus consistent with metastasis in the left lobe (arrow in 7d) and bilateral small reactive pleural effusion (7b and 7c).**

explanation may be applied to humans. Besides radiation, some of these changes may also be attributed to the embolic effect of the microspheres. Studies based on TACE have shown that, after arterial embolization, some of the embolic particles may reach the portal venules through the transplexal route. This could cause simultaneous arterial and venous obliteration, leading to parenchymal infarcts that tend to gradually recover through arterial recanalization and collateralization[34]. Arterial reperfusion of infarcted parenchyma would also cause inhomogeneous enhancement on post-contrast CT and MR studies. The size range of commercially available ^{90}Y microspheres is smaller than the particles used in TACE and hence it is eminently feasible for simultaneous arterial and venous occlusion and their sequelae to be seen after ^{90}Y treatment.

Volumetric changes

Volumetric changes in the liver after radioembolization, such as ipsilateral hepatic lobar volume decrease, contralateral lobar hypertrophy, as well as induction of liver fibrosis and portal hypertension can occur without clinical sequelae[36]. At a mean follow-up interval of 139 days, Jakobs et al.[36] found a mean decrease in liver volume of 11.8% with sequential bilobar treatment and 8.9% ipsilateral lobar volume decrease with a 21.2% increase in the volume of the contralateral lobe in patients receiving unilobar treatment. In patients receiving bilobar treatment, they noted findings of portal hypertension with the mean volume of the spleen increasing by around 28% along with an increase in the diameter of the main portal vein, superior mesentric vein and splenic vein.

In patients receiving unilobar treatment, the portal vein in the ipsilateral lobe would be smaller in caliber with an increase in the diameter of the contralateral intrahepatic portal vein with no significant increase in splenic vein diameter. These findings strongly suggest fibrotic remodeling of the treated liver. The atrophy of the treated lobe can be seen due to a direct effect of the radiation and embolization of vessels; the hypertrophy of the contralateral lobe may be a compensatory phenomenon associated with alteration in blood flow.

Based on a longer follow-up, a protracted form of the above volumetric changes was described by Gaba et al.[37]. They coined the term radiation lobectomy to describe the phenomenon of marked reduction in ipsilateral hepatic volume and contralateral volume expansion after ^{90}Y therapy. At a mean follow-up interval of 18 months, they found 52% reduction in the volume of the treated right lobe and a 40% increase in the volume of the contralateral left lobe. None of their patients had any hepatic insufficiency. In the experience of these investigators, the incidence of radiation lobectomy in patients with unilobar right lobe disease was 19.8%. In this cohort, the tumors (HCC) showed better response to treatment. Their survival was better with 46% 5-year survival and a median survival of 36.6 months, which is comparable with the 33–50% survival rates reported after curative surgical resection[37,38].

Capsular retraction

Radioembolization can cause capsular retraction that mimics cirrhosis in an otherwise non-cirrhotic liver (Fig. 8)[30]. This is more often seen in patients with diffuse multifocal disease. Young et al.[39] described a similar appearance in patients who had received chemotherapy for multiple liver metastases from breast carcinoma. They attributed the findings to shrinkage of the tumor with resultant scar formation and nodular regenerative hyperplasia of the intervening uninvolved areas. Atassi et al.[30] extrapolates the same pathogenesis to the capsular retraction seen after ^{90}Y therapy, besides the obvious contribution from radiation-induced fibrosis of hepatic parenchyma.

Perihepatic fluid and pleural effusions

TARE aims to provide a tumoricidal dose of around 100 Gy to the hepatic tumor while keeping the exposure of normal hepatocytes to a minimum; preferably below 40–60 Gy[40,41]. In patients with multifocal tumors for whom selective injection is not possible and when the tumor/normal liver ratio is low, higher doses of radiation energy may get delivered to non-tumorous liver. In such a scenario, it is natural for the structures around the liver to receive variable amounts of radiation from the ^{90}Y particles trapped within the adjacent liver. After radioembolization, a sliver of perihepatic fluid is seen in 20% of patients; this could be a reaction to the irradiation of the Glisson capsule (Fig. 8). Similar reactionary changes in the pleural space may manifest as pleural effusion[30] (Fig. 7). Such findings are often self-limiting and they only require symptomatic treatment.

Complications

Biliary complications

In the early days of TARE, the most common complications were due to non-targeted embolization. However, with refining of techniques, now the most common complications are biliary in nature. After radioembolization, biliary complications such as biliary dilatation, biloma, cholecystitis and cholangitis may be expected in up to 10% of patients[42]. Unlike hepatic parenchyma, the biliary tree lacks dual blood supply. The common hepatic duct and supraduodenal common bile duct are supplied by the gastroduodenal artery in 62% of people and by the right hepatic artery in the remaining 38%. The right and left hepatic ducts are supplied by accompanying hepatic arteries, whereas the intrahepatic biliary tree is perfused by the peribiliary vascular plexus that is exclusively fed by hepatic arterial branches[43]. This explains the susceptibility of the biliary tree to ischemic injury after transarterial therapies to the liver. The diameter of the blood vessels constituting the peribiliary plexus is in the range of 20–60 μm. This enables the microspheres used in TARE, which are usually 20–40 μm, to get trapped in these vessels and cause both ischemia and radiation-induced biliary necrosis. A cirrhotic liver has hypertrophy of the peribiliary plexus; thus it is at lower risk of biliary necrosis than a non-cirrhotic liver, after radioembolization[44]. This is reflected in the higher incidence of biliary complications when TARE is performed for hepatic metastasis rather than for HCC[42].

In the acute stage of bile duct injury, biliary necrosis is seen as small cystic structures, often in clusters around a necrotic tumor, adjacent to a portal venous branch and usually within the distribution of the embolized artery (Fig. 9). Subsequently they rupture, leaking bile along the Glisson sheath, causing coagulation necrosis of the adjacent hepatic parenchyma and thrombosis of the small arterial vessels in the vicinity. The leaking bile accumulates to form a biloma (Fig. 9). A biloma may be seen as a large well-defined solitary or multiple fluid-filled lesion with or without segmental bile duct dilatation; a branching pattern of hypoattenuation along the Glisson sheath with a beaded appearance and simulating dilatation of the intrahepatic biliary tree; or a subcapsular fluid collection with density similar to bile duct. Most of them develop within the first 2 months after the procedure. A communication between the biloma and the biliary tree is rarely demonstrable; however, cholangiography may show a proximal stricture of the draining intrahepatic duct. The presence of rim enhancement around a biloma is not unusual and it does not always indicate

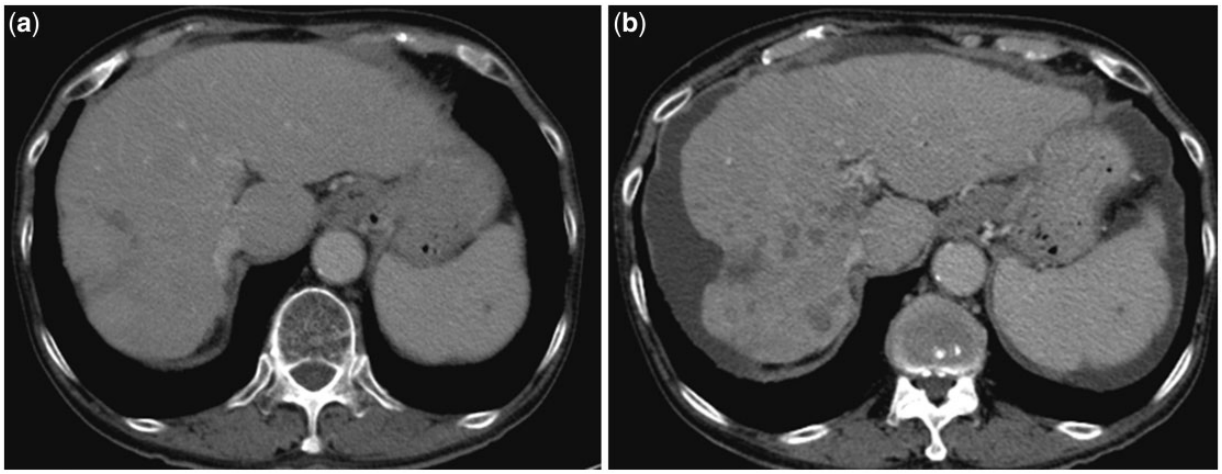

Figure 8 **Pre-treatment CT scan (8a) in a patient with multiple hepatic metastases shows normal shape and contour of the liver. CT scan obtained 2 months after bilobar ^{90}Y radioembolization (8b) shows generalized hepatic atrophy with irregular surface. An area of prominent capsular surface retraction is noted at the dome of the right lobe. Note the several non-enhancing, ill-defined hypodense areas in the right lobe, representing areas of scarring or small bilomas. A sliver of perihepatic fluid is seen. Despite these morphological changes, this patient had normal synthetic function of the liver.**

infection. Stricture and dilatation of the bile duct usually indicates chronic-stage bile duct injury. Most of these biliary complications are asymptomatic. Treatment is required only if they clinically manifest or get secondarily infected. Indolent large bilomas may shrink and even resolve completely or stabilize over time[42,45–47].

TARE-related acute cholecystitis may occur due to microspheres embolizing the cystic artery or due to direct radiation injury from accumulation of ^{90}Y particles in the adjacent liver parenchyma. Typical radiologic findings include abnormal gallbladder wall enhancement with edema and/or disruption and/or pericholecystic fluid on CT/MR imaging[42]. Unlike in the normal population, these radiologic findings have very limited prognostic value in patients who have recently undergone radioembolization. If the patient is clinically well, radiologic evidence of acute cholecystitis or even obvious gall bladder wall perforation does not merit active management. Less than 1% of patients with radiation cholecystitis require surgical intervention[47].

Hepatic abscess

As seen with TACE and other embolotherapies, hepatic abscess is a potential complication after ^{90}Y therapy. Hepatic abscess may be an infected biloma or secondary to infection of a necrotic tumor. Because ascending infection is the easiest route for microorganisms to access the hepatic parenchyma, the presence of a bilioenteric anastomosis is a strong predisposing factor, with hepatic abscess seen in up to 25% of such patients compared with less than 1% of patients who have an intact sphincter of Oddi[48]. Prophylactic antibiotics and bowel cleansing may decrease this risk. The presence of an obstructed biliary system is another risk factor for hepatic abscess formation. In a routine patient, rim-enhancing fluid collection in the liver, with/without pockets of air is almost pathognomonic of a liver abscess. However, this interpretation must be made with great caution in a patient on post-TARE follow-up because tumor necrosis with surrounding reactionary changes is also seen as a rim-enhancing fluid collection. Similarly, locules of air are often seen within the liver after a recent embolization; most of this air gains entry into the liver trapped in between the embolic particles[49]. Even bilomas can mimic an abscess. Hence, it is essential to interpret the imaging features in the light of the patient's clinical syndrome and perform a diagnostic aspiration whenever there is doubt.

Radioembolization-induced liver disease

Radioembolization-induced liver disease (REILD) is a potentially life-threatening, radiation-induced, subacute liver injury in the same league as radiation inducted liver disease, which follows external irradiation of liver tumors and combined modality-induced liver disease encountered in patients receiving allogenic bone marrow transplantation when high-dose chemotherapy and total-body irradiation are used as preparative procedures. REILD is characterized by jaundice and ascites developing 4−8 weeks after treatment, in the absence of overt biliary dilatation or tumor progression with increase in total bilirubin, increasing alkaline phosphatase and γ-glutamyl transpeptidase, and no changes in transaminases. The pathologic changes include extensive sinusoidal congestion affecting perivenular areas with focal hepatic atrophy, areas of necrosis around central

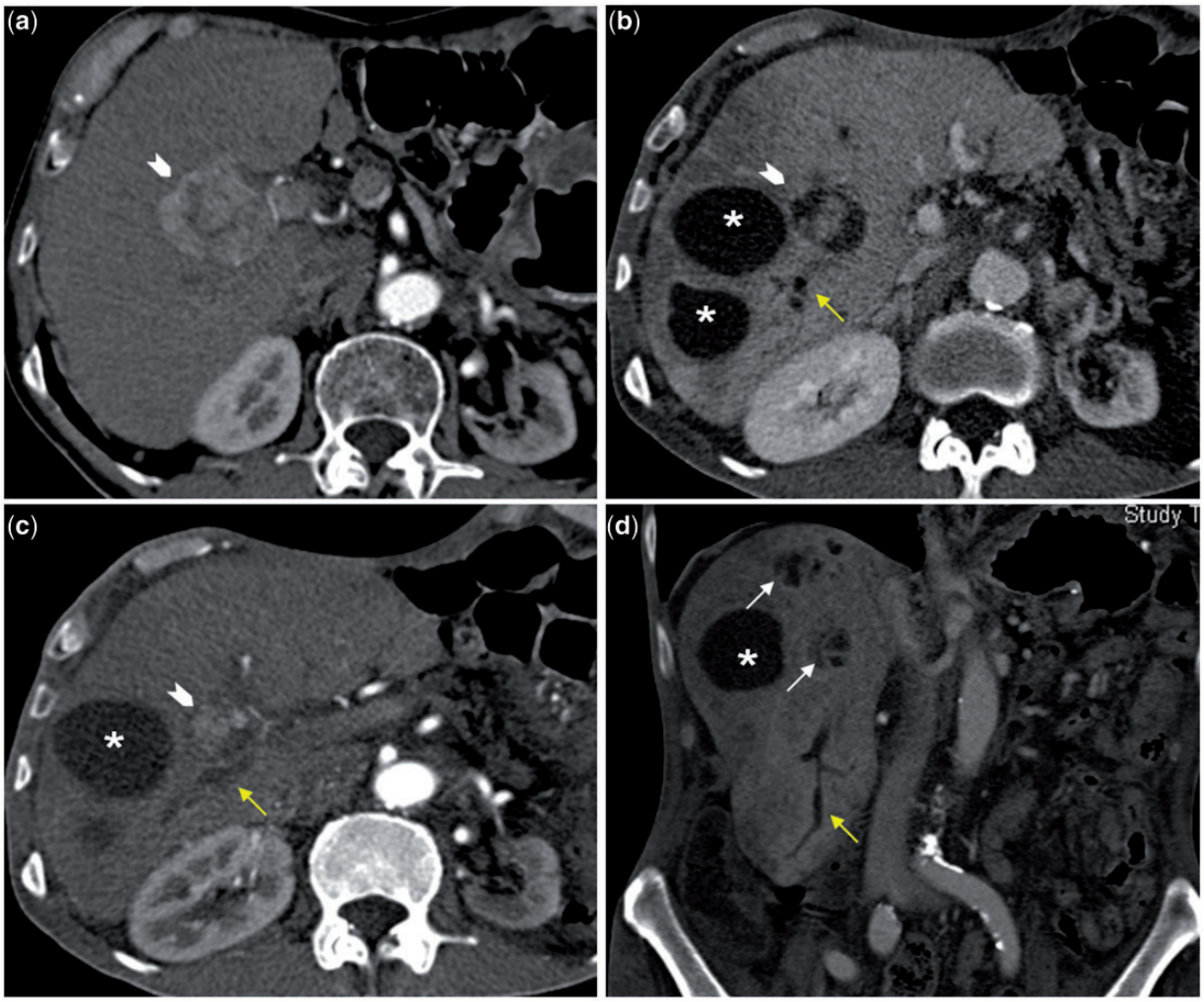

Figure 9 **This arterial phase CT scan (9a) shows a hypervascular tumor (arrowhead). Post-TARE arterial (9c) and portovenous (9b) phase CT scans show marked decrease in the size of the tumor with areas of necrosis around the residual tumor. The large, well-defined fluid-filled areas (asterisk) seen in 9b–d represent bilomas. The coronal image shows two clusters of smaller fluid density areas (white arrows); these represent foci of biliary necrosis that may coalesce to form a biloma. Also note the segmental biliary dilatation (yellow arrows) suggesting the presence of biliary strictures. Hepatic parenchyma appears heterogeneous in the portovenous phase with ill-defined geographic areas of hypodensity.**

veins with fresh thrombosis, and some cholestasis in periportal areas, consistent with veno-occlusive disease[50]. The overall incidence of REILD after ^{90}Y administration ranges from 4% to 9%[51,52]; however, in patients who have received heavy pre-treatment with chemotherapeutic agents, this may go up to 20%[50]. The radiologic findings are non-specific and include parenchymal edema with transient hepatomegaly, progressing to subcapsular edema and ascites. The diagnosis is essentially clinical and the role of radiology is predominantly to exclude other causes such as biliary obstruction or tumor progression.

Gastrointestinal complications

After TARE, gastrointestinal complications such as gastric and duodenal ulcers, hollow viscus perforation and pancreatitis have been described. Most of these are caused by non-targeted embolization with the microspheres reaching unintended locations[30]. Imaging findings are non-specific and they depend on the organ affected. Post-TARE pancreatitis most often affects the head of the pancreas. Even in the absence of non-targeted embolization, if the microspheres are lodged in the periphery of the liver, the neighboring viscera will receive some irradiation. The gastrointestinal tract is most often affected in this manner and the most common manifestation is radiation gastritis of variable severity[53].

Radiation pneumonitis

Radiation pneumonitis is a potential complication of TARE due to shunting of the microspheres from the hepatic to the pulmonary circulation. Meticulous

estimation of the lung shunt fraction before treatment can usually prevent this complication. Radiographically, it presents 1–2 months after therapy as ill-defined patchy opacities and ground glass nodularity in a symmetric pattern with relative hilar/perihilar sparing. It can also resemble an organizing or chronic eosinophilic pneumonia. These changes can resolve or may progress to fibrosis, traction bronchiectasis and focal honey combing[47,54].

Conclusion

Evaluation of the therapeutic effect of TARE on liver tumors is primarily based on radiologic imaging. However, the quality of evidence regarding the clinical significance and pathologic basis of the radiologic findings seen at post-TARE follow-up is suboptimal. They are mostly based on small cohort studies and retrospective analysis. The inherent nature of the treatment, and the stage of disease for which it is most extensively used, probably constitute the greatest barrier in gathering this information. There is an overwhelming need for large prospective studies in order to recognize and confirm new response criteria as well as imaging biomarkers.

Reduction in tumor size, necrosis and lack of tumor enhancement as seen at CT and MRI are primary surrogates of a favorable response to ^{90}Y treatment. Use of PET/CT and functional MR imaging techniques such as DWI can be helpful in solving certain diagnostic dilemmas that may be encountered during post-TARE follow-up imaging. Radiologists need to be aware of certain benign findings that are unique to post-TARE livers, such as peritumoral edema, perilesional thin rim of enhancement and geographic areas of hypodensity in non-tumorous liver. This knowledge would ensure that there is a low rate of false-positive diagnosis of progressive disease. Similarly, knowledge of the common complications that follow ^{90}Y treatment and their pathogenesis would empower the radiologist in generating more informed and intelligent impressions from their observations.

Conflict of interest

The authors have no conflicts of interest to declare.

References

[1] Breedis C, Young G. The blood supply of neoplasms in the liver. Am J Pathol 1954; 30: 969–977. PMid:13197542.

[2] Lien WM, Ackerman NB. The blood supply of experimental liver metastases. II. A microcirculatory study of the normal and tumor vessels of the liver with the use of perfused silicone rubber. Surgery 1970; 68: 334–340. PMid:5450714.

[3] Kennedy AS, Nutting C, Coldwell D, Gaiser J, Drachenberg C. Pathologic response and microdosimetry of (90)Y microspheres in man: review of four explanted whole livers. Int J Radiat Oncol Biol Phys 2004; 60: 1552–1563. PMid:15590187.

[4] Kennedy A, Nag S, Salem R, et al. Recommendations for radioembolization of hepatic malignancies using yttrium-90 microsphere brachytherapy: a consensus panel report from the radioembolization brachytherapy oncology consortium. Int J Radiat Oncol Biol Phys 2007; 68: 13–23. PMid:17448867.

[5] Sarfaraz M, Kennedy AS, Lodge MA, Li XA, Wu X, Yu CX. Radiation absorbed dose distribution in a patient treated with yttrium-90 microspheres for hepatocellular carcinoma. Med Phys 2004; 31: 2449–2453. PMid:15487724.

[6] Inarrairaegui M, Pardo F, Bibao JI, et al. Response to radioembolization with yttrium 90 resin microspheres may allow surgical treatment with curative intent and prolonged survival in previously unresectable hepatocellular carcinoma. Eur J Surg Oncol 2012; 38: 594–601. PMid:22440743.

[7] Salem R, Thurston KG, Carr BI, Goin JE, Geschwind JF. Yttrium-90 microspheres: radiation therapy for unresectable liver cancer. J Vasc Interv Radiol 2002; 13: 9 Pt 2S223–229. PMid:12354840.

[8] Hilgard P, Hamami M, Fouly AE, et al. Radioembolization with yttrium-90 glass microspheres in hepatocellular carcinoma: European experience on safety and long term survival. Hepatology 2010; 52: 1741–1749. PMid:21038413.

[9] Evans KA, Richardson MG, Pavlakis N, Morris DL, Liauw W, Bester L. Survival outcomes of a salvage patient population after radioembolization of hepatic metastasis with yttrium-90 microspheres. J Vasc Interv Radiol 2010; 21: 1521–1526. PMid:20813542.

[10] Miller AB, Hoogstraten B, Staquet M, Winkler A. Reporting results of cancer treatment. Cancer 1981; 47: 207–214. PMid:7459811.

[11] Therasse P, Arbuck SG, Eisenhauer EA, et al. New guidelines to evaluate the response to treatment in solid tumors. European Organization for Research and Treatment of Cancer, National Cancer Institute of the United States, National Cancer Institute of Canada. J Natl Cancer Inst 2000; 92: 205–216. PMid:10655437.

[12] European Association for the Study of the Liver; European Organisation for Research and Treatment of Cancer. EASL-EORTC clinical practice guidelines: management of hepatocellular carcinoma. J Hepatol 2012; 56: 908–943. PMid:22424438.

[13] Lencioni R, Llovet JM. Modified RECIST (mRECIST) assessment for hepatocellular carcinoma. Semin Liver Dis 2010; 30: 52–60. PMid:20175033.

[14] Bruix J, Sherman M, Llovet JM, et al. Clinical management of hepatocellular carcinoma. Conclusions of the Barcelona-2000 EASL conference. J Hepatol 2001; 35: 421–430. PMid:11592607.

[15] Keppke AL, Salem R, Reddy D, et al. Imaging of hepatocellular carcinoma after treatment with yttrium-90 microspheres. AJR Am J Roentgenol 2007; 188: 768–775. PMid:17312067.

[16] Miller FH, Keppke AL, Reddy D, et al. Response of liver metastasis after treatment with yttrium-90 microspheres: role of size, necrosis and PET. AJR Am J Roentgenol 2007; 188: 776–783. PMid:17312068.

[17] Sato K, Lewandowski RJ, Bui JT, et al. Treatment of unresectable primary and metastatic liver cancer with yttrium-90 microspheres (Therasphere): assessment of hepatic arterial embolization. Cardiovasc Intervent Radiol 2006; 29: 522–529. PMid:16729228.

[18] Llovet JM, Di Bisceglie AM, Bruix J, et al. Panel of Experts in HCC-Design Clinical Trials. Design and endpoints of clinical trials in hepatocellular carcinoma. J Natl Cancer Inst 2008; 100: 698–711. PMid:18477802.

[19] Salem R, Thurston KG. Radioembolization with 90Yttrium microspheres: a state-of-the-art brachytherapy treatment for primary and secondary liver malignancies. Part 1: technical and methodologic considerations. J Vasc Interv Radiol 2006; 17: 1251–1278. PMid:16923973.

[20] Wong CY, Salem R, Raman S, Gates VL, Dworkin HJ. Evaluating ^{90}Y-glass microsphere treatment response on unresectable colorectal liver metastases by [^{18}F] FDG PET: a comparison

with CT or MRI. Eur J Nucl Med Mol Imaging 2002; 29: 815–820. PMid:12029557.

[21] Bester L, Hobbins PG, Wang SC, Salem R. Imaging characteristics following 90yttrium microsphere treatment for unresectable liver cancer. J Med Imaging Radiat Oncol 2011; 55: 111–118. PMid:21501398.

[22] Sacks A, Peller PJ, Surasi DS, Chatburn L, Mercier G, Subramaniam RM. Value of PET/CT in the management of liver metastases, Part 1. AJR Am J Roentgenol 2011; 197: W256–259. PMid:21785050.

[23] Antoch G, Vogt FM, Veit P, et al. Assessment of liver tissue after radiofrequency ablation: findings with different imaging procedures. J Nucl Med 2005; 46: 520–525. PMid:15750168.

[24] Wong CY, Qing F, Savin M, et al. Reduction of metastatic load to tumor after intraarterial hepatic yttrium-90 radioembolization as evaluated by [^{18}F]fluorodeoxyglucose positron emission tomographic imaging. J Vasc Interv Radiol 2005; 16: 1101–1106. PMid:16105922.

[25] Khan MA, Combs CS, Brunt EM, et al. Positron emission tomography scanning in the evaluation of hepatocellular carcinoma. J Hepatol 2000; 32: 792–797. PMid:10845666.

[26] Kamel IR, Bluemke DA. Imaging evaluation of hepatocellular carcinoma. J Vasc Interv Radiol 2002; 13(9 Pt2): S173–184. PMid:12354834.

[27] Kuszyk BS, Boitnott JK, Choti MA, et al. Local tumor recurrence following hepatic cryoablation: radiologic-histopathologic correlation in a rabbit model. Radiology 2000; 217: 477–486. PMid:11058649.

[28] Rhee TK, Naik NK, Deng J, et al. Tumor response after yttrium-90 radioembolization for hepatocellular carcinoma: comparison of diffusion weighted functional MR imaging with anatomic MR imaging. J Vasc Interv Radiol 2008; 19: 1180–1186. PMid:18656011.

[29] Deng J, Miller FH, Rhee TK, et al. Diffusion weighted MR imaging for determination of hepatocellular carcinoma response to yttrium-90 radioembolization. J Vasc Interv Radiol 2006; 17: 1195–1200. PMid:16868174.

[30] Atassi B, Bangash AK, Bahrani A, et al. Multimodality imaging following 90Y radioembolization: a comprehensive review and pictorial essay. Radiographics 2008; 28: 81–99. PMid:18203932.

[31] Ibrahim SM, Nikolaidis P, Miller FH, et al. Radiologic findings following Y90 radioembolization for primary liver malignancies. Abdom Imaging 2009; 34: 566–581. PMid:18777189.

[32] Kulik LM, Atassi B, Van Holsbeeck L, et al. Yttrium-90 microspheres (Therasphere) treatment of unresectable hepatocellular carcinoma: downstaging to resection, RFA and bridge to transplantation. J Surg Oncol 2006; 94: 572–586. PMid:17048240.

[33] Wollner I, Knutsen C, Smith P, et al. Effects of hepatic arterial yttrium 90 glass microspheres in dogs. Cancer 1988; 61: 1336–1344. PMid:3345490.

[34] Chung J, Yu JS, Chung JJ, Kim JH, Kim KW. Haemodynamic events and localized parenchymal changes following transcatheter arterial chemoembolisation for hepatic malignancy: interpretation of imaging findings. Br J Radiol 2010; 83: 71–81. PMid:19581309.

[35] Murthy R, Nunez R, Szklaruk J, et al. Yttrium-90 microsphere therapy for hepatic malignancy: devices, indications, technical considerations, and potential complications. Radiographics 2005; 25(Suppl 1): S41–55. PMid:16227496.

[36] Jakobs TF, Saleem R, Atassi B, et al. Fibrosis, portal hypertension, and hepatic volume changes induced by intra-arterial radiotherapy with 90yttrium microspheres. Dig Dis Sci 2008; 53: 2556–2563. PMid:18231857.

[37] Gaba RC, Lewandowski RJ, Kulik LM, et al. Radiation Lobectomy: preliminary findings of hepatic volumetric response to lobar yttrium-90 radioembolization. Ann Surg Oncol 2009; 16: 1587–1596. PMid:19357924.

[38] Roxburgh P, Evans TR. Systemic therapy of hepatocellular carcinoma: are we making progress? Adv Ther 2008; 25: 1089–1104. PMid:18972075.

[39] Young ST, Paulson EK, Washington K, Gulliver DJ, Vredenburgh JJ, Baker ME. CT of the liver in patients with metastatic breast carcinoma treated by chemotherapy: findings simulating cirrhosis. AJR Am J Roentgenol 1994; 163: 1385–1388. PMid:7992734.

[40] Gil-Alzugaray B, Chopitea A, Iñarrairaegui M, et al. Prognostic factors and prevention of radioembolization-induced liver disease. Hepatology 2013; 57: 1078–1087. PMid:23225191.

[41] Ho S, Lau WY, Leung TWT, Johnson PJ. Internal radiation therapy for patients with primary or metastatic hepatic cancer. Cancer 1998; 83: 1894–1907. PMid:9806647.

[42] Attassi B, Bangash AK, Lewandowski RJ, et al. Biliary sequelae following radioembolization with Yttrium-90 microspheres. J Vasc Interv Radiol 2008; 19: 691–697.

[43] Northover JM, Terblanche J. A new look at the arterial supply of the bile duct in man and its surgical implications. Br J Surg 1979; 66: 379–384. PMid:466017.

[44] Yu JS, Kim KW, Jeong MG, Lee DH, Park MS, Yoon SW. Predisposing factors of bile duct injury after transcatheter arterial chemoembolization (TACE) for hepatic malignancy. Cardiovasc Intervent Radiol 2002; 25: 270–274. PMid:12042987.

[45] Chung J, Yu JS, Chung JJ, Kim JH, Kim KW. Haemodynamic events and localized parenchymal changes following transcatheter arterial chemoembolisation for hepatic malignancy: interpretation of imaging findings. Br J Radiol 2010; 83: 71–81. PMid:19581309.

[46] Sakamoto I, Iwanaga S, Nagaoki K, et al. Intrahepatic biloma formation (bile duct necrosis) after transcatheter arterial chemoembolization. AJR Am J Roentgenol 2003; 181: 79–87. PMid:12818833.

[47] Riaz A, Lewandowski RJ, Kulik LM, et al. Complications following radioembolization with yttrium-90 microspheres: a comprehensive literature review. J Vasc Interv Radiol 2009; 20: 1121–1130. PMid:19640737.

[48] Brown DB, Cardella JF, Sacks D, et al. Quality improvement guidelines for transhepatic arterial chemoembolization, embolization, and chemotherapeutic infusion for hepatic malignancy. J Vasc Interv Radiol 2009; 20(7 Suppl): S219–S226, S226.e1–10. PMid:19560002.

[49] Clark TW. Complications of hepatic chemoembolization. Semin Intervent Radiol 2006; 23: 119–125. PMid:21326755.

[50] Sangro B, Gil-Alzugaray B, Rodriguez J, et al. Liver disease induced by radioembolization of liver tumors: description and possible risk factors. Cancer 2008; 112: 1538–1546. PMid:18260156.

[51] Lim L, Gibbs P, Yip D, et al. Prospective study of treatment with selective internal radiation therapy spheres in patients with unresectable primary or secondary hepatic malignancies. Intern Med J 2005; 35: 222–227. PMid:15836500.

[52] Sharma RA, Van Hazel GA, Morgan B, et al. Radioembolization of liver metastases from colorectal cancer using yttrium-90 microspheres with concomitant systemic oxaliplatin, fluorouracil, and leucovorin. J Clin Oncol 2007; 25: 1099–1106. PMid:17369573.

[53] Ahmadzadehfar H, Biersack HJ, Ezziddin S. Radioembolization of liver tumors with yttrium-90 microspheres. Semin Nucl Med 2010; 40: 105–121. PMid:20113679.

[54] Wright CL, Werner JD, Tran JM, et al. Radiation pneumonitis following yttrium-90 radioembolization: case report and literature review. J Vasc Interv Radiol 2012; 23: 669–674. PMid:22525023.